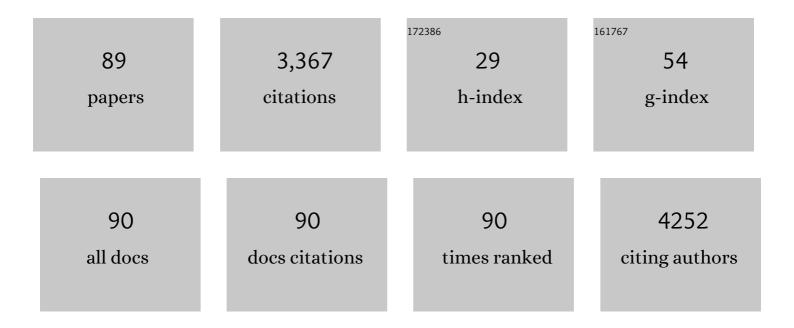
## Le Zhou

## List of Publications by Year in descending order

Source: https://exaly.com/author-pdf/1594177/publications.pdf Version: 2024-02-01



#	Article	IF	CITATIONS
1	Elimination of extraordinarily high cracking susceptibility of aluminum alloy fabricated by laser powder bed fusion. Journal of Materials Science and Technology, 2022, 103, 50-58.	5.6	21
2	Microstructural Development in Inconel 718 Nickel-Based Superalloy Additively Manufactured by Laser Powder Bed Fusion. Metallography, Microstructure, and Analysis, 2022, 11, 88-107.	0.5	16
3	Microstructural characteristics and mechanical properties of additively manufactured Cu–10Sn alloys by laser powder bed fusion. Materials Science & Engineering A: Structural Materials: Properties, Microstructure and Processing, 2022, 838, 142775.	2.6	12
4	Effect of functionality of thiol on the optical properties of liquid crystals/polymer composite films. Liquid Crystals, 2021, 48, 313-321.	0.9	10
5	Oxygen-assisted direct growth of large-domain and high-quality graphene on glass targeting advanced optical filter applications. Nano Research, 2021, 14, 260-267.	5.8	20
6	Effects of Alloy Composition and Solid-State Diffusion Kinetics on Powder Bed Fusion Cracking Susceptibility. Journal of Phase Equilibria and Diffusion, 2021, 42, 5-13.	0.5	17
7	Effects of the methacrylate monomers with different end groups on the morphologies, electro-optical and mechanical properties of polymer dispersed liquid crystals composite films. Liquid Crystals, 2021, 48, 722-734.	0.9	26
8	Microstructural Development in As Built and Heat Treated IN625 Component Additively Manufactured by Laser Powder Bed Fusion. Journal of Phase Equilibria and Diffusion, 2021, 42, 14-27.	0.5	21
9	<i>In situ</i> TEM Characterization of Microstructure Evolution and Mechanical Behavior of the 3D-Printed Inconel 718 Exposed to High Temperature. Microscopy and Microanalysis, 2021, 27, 250-256.	0.2	7
10	Effects of multifunctional acrylates and thiols on the morphology and electro-optical properties of polymer-dispersed liquid crystal films. Liquid Crystals, 2021, 48, 1457-1466.	0.9	17
11	Composition-dependent solidification cracking of aluminum-silicon alloys during laser powder bed fusion. Acta Materialia, 2021, 208, 116698.	3.8	97
12	High strength WE43 microlattice structures additively manufactured by laser powder bed fusion. Materialia, 2021, 16, 101067.	1.3	18
13	The Electro-Optical Properties and Adhesion Strength of Epoxy-Polymercaptan-Based Polymer Dispersed Liquid Crystal Films. Crystals, 2021, 11, 576.	1.0	8
14	Additive manufacturing and mechanical properties of the dense and crack free Zr-modified aluminum alloy 6061 fabricated by the laser-powder bed fusion. Additive Manufacturing, 2021, 41, 101966.	1.7	28
15	High throughput mechanical testing platform and application in metal additive manufacturing and process optimization. Journal of Manufacturing Processes, 2021, 66, 494-505.	2.8	9
16	Design of heterogeneous structured Al alloys with wide processing window for laser-powder bed fusion additive manufacturing. Additive Manufacturing, 2021, 42, 102002.	1.7	10
17	Microstructure, mechanical performance, and corrosion behavior of additively manufactured aluminum alloy 5083 with 0.7 and 1.0Âwt% Zr addition. Materials Science & Engineering A: Structural Materials: Properties, Microstructure and Processing, 2021, 823, 141679.	2.6	36
18	Mechanical Behavior Assessment of Ti-6Al-4V ELI Alloy Produced by Laser Powder Bed Fusion. Metals, 2021, 11, 1671.	1.0	15

Lе Zнои

#	Article	IF	CITATIONS
19	An integrated computational materials engineering-anchored closed-loop method for design of aluminum alloys for additive manufacturing. Materialia, 2020, 9, 100574.	1.3	40
20	Optical diffusers based on uniform nano-sized polymer balls/nematic liquid crystals composite films. Liquid Crystals, 2020, 47, 785-798.	0.9	10
21	Anomalous growth of Al8Mo3 phase during interdiffusion and reaction between Al and Mo. Journal of Nuclear Materials, 2020, 539, 152337.	1.3	9
22	Laser powder bed fusion of Al–10 wt% Ce alloys: microstructure and tensile property. Journal of Materials Science, 2020, 55, 14611-14625.	1.7	51
23	Recent Advances in The Polymer Dispersed Liquid Crystal Composite and Its Applications. Molecules, 2020, 25, 5510.	1.7	84
24	Effect of Polymer Network Topology on the Electroâ€Optical Performance of Polymer Stabilized Liquid Crystal (PSLC) Devices. Macromolecular Chemistry and Physics, 2020, 221, 2000185.	1.1	23
25	Ligand assisted swelling–deswelling microencapsulation (LASDM) for stable, color tunable perovskite–polymer composites. Nanoscale Advances, 2020, 2, 2034-2043.	2.2	21
26	Understanding the Laser Powder Bed Fusion of AlSi10Mg Alloy. Metallography, Microstructure, and Analysis, 2020, 9, 484-502.	0.5	67
27	Additive manufacturing of dense WE43 Mg alloy by laser powder bed fusion. Additive Manufacturing, 2020, 33, 101123.	1.7	30
28	Process-Dependent Composition, Microstructure, and Printability of Al-Zn-Mg and Al-Zn-Mg-Sc-Zr Alloys Manufactured by Laser Powder Bed Fusion. Metallurgical and Materials Transactions A: Physical Metallurgy and Materials Science, 2020, 51, 3215-3227.	1.1	48
29	Effects of rigid structures containing (meth)acrylate monomers and crosslinking agents with different chain length on the morphology and electro-optical properties of polymer-dispersed liquid crystal films. Journal of Modern Optics, 2020, 67, 682-691.	0.6	23
30	The fabrication of novel optical diffusers based on UV-cured polymer dispersed liquid crystals. Liquid Crystals, 2019, 46, 138-144.	0.9	26
31	Microstructure and tensile property of a novel AlZnMgScZr alloy additively manufactured by gas atomization and laser powder bed fusion. Scripta Materialia, 2019, 158, 24-28.	2.6	158
32	Numerical simulation of high-pressure gas atomization of two-phase flow: Effect of gas pressure on droplet size distribution. Advanced Powder Technology, 2019, 30, 2726-2732.	2.0	34
33	The effective control of Cu through-silicon via extrusion for three-dimensional integrated circuits by a metallic cap layer. Scripta Materialia, 2019, 164, 101-104.	2.6	7
34	65â€3: Light Diffusing, Down onverting Perovskiteâ€onâ€Polymer Microspheres. Digest of Technical Papers SID International Symposium, 2019, 50, 917-920.	0.1	0
35	Microstructure and mechanical properties of Zr-modified aluminum alloy 5083 manufactured by laser powder bed fusion. Additive Manufacturing, 2019, 28, 485-496.	1.7	60
36	A switchable optical diffuser based on a polymer/nematic liquid crystal composite film with transient polymer balls-networks microstructure. Liquid Crystals, 2019, 46, 2213-2222.	0.9	11

LE ZHOU

#	Article	IF	CITATIONS
37	Fabrication of a controllable anti-peeping device with a laminated structure of microlouver and polymer dispersed liquid crystals film. Liquid Crystals, 2019, 46, 2235-2244.	0.9	25
38	Light diffusing, down-converting perovskite-on-polymer microspheres. Journal of Materials Chemistry C, 2019, 7, 6527-6533.	2.7	15
39	Switchable anti-peeping film for liquid crystal displays from polymer dispersed liquid crystals. Liquid Crystals, 2019, 46, 718-724.	0.9	25
40	Phase Transformations and Microstructural Development in the U-10 WtÂPct Mo Alloy with Varying Zr Contents After Heat Treatments Relevant to the Monolithic Fuel Plate Fabrication Process. Metallurgical and Materials Transactions A: Physical Metallurgy and Materials Science, 2019, 50, 72-96.	1.1	9
41	Microstructure, precipitates and mechanical properties of powder bed fused inconel 718 before and after heat treatment. Journal of Materials Science and Technology, 2019, 35, 1153-1164.	5.6	94
42	Microstructure, precipitates and hardness of selectively laser melted AlSi10Mg alloy before and after heat treatment. Materials Characterization, 2018, 143, 5-17.	1.9	201
43	Enhancing Electron Transfer and Electrocatalytic Activity on Crystalline Carbon-Conjugated g-C <sub>3</sub> N <sub>4</sub> . ACS Catalysis, 2018, 8, 1926-1931.	5.5	172
44	Holey Films: Freestanding NiFe Oxyfluoride Holey Film with Ultrahigh Volumetric Capacitance for Flexible Asymmetric Supercapacitors (Small 3/2018). Small, 2018, 14, 1870014.	5.2	1
45	Effects of Degassing on the Microstructure, Chemistry, and Estimated Mechanical Properties of a Cryomilled Al-Mg Alloy. Metallurgical and Materials Transactions A: Physical Metallurgy and Materials Science, 2018, 49, 3066-3079.	1.1	1
46	Phosphorus and Aluminum Codoped Porous NiO Nanosheets as Highly Efficient Electrocatalysts for Overall Water Splitting. ACS Energy Letters, 2018, 3, 892-898.	8.8	130
47	Effects of crosslinking agent/diluents/thiol on morphology of the polymer matrix and electro-optical properties of polymer-dispersed liquid crystal. Liquid Crystals, 2018, 45, 728-735.	0.9	36
48	MoS <sub>2</sub> /TiO <sub>2</sub> heterostructures as nonmetal plasmonic photocatalysts for highly efficient hydrogen evolution. Energy and Environmental Science, 2018, 11, 106-114.	15.6	326
49	Surfaceâ€Modified Porous Carbon Nitride Composites as Highly Efficient Electrocatalyst for Znâ€Air Batteries. Advanced Energy Materials, 2018, 8, 1701642.	10.2	129
50	Preparation of polymer-dispersed liquid crystal doped with indium tin oxide nanoparticles. Liquid Crystals, 2018, 45, 1068-1077.	0.9	23
51	Freestanding NiFe Oxyfluoride Holey Film with Ultrahigh Volumetric Capacitance for Flexible Asymmetric Supercapacitors. Small, 2018, 14, 1702295.	5.2	34
52	Diffusion and its Application in NiMnGa Alloys. , 2018, 19, 80-95.		1
53	A novel optical diffuser based on polymer micro-balls-filled nematic liquid crystal composite film. RSC Advances, 2018, 8, 40347-40357.	1.7	15
54	18â€4: Converting Light Diffusing Polymer Powders into Stable Perovskiteâ€Based Tunable Downconverters. Digest of Technical Papers SID International Symposium, 2018, 49, 222-224.	0.1	5

LE ZHOU

#	Article	IF	CITATIONS
55	Noncontact stress measurement from bare <scp>UHPC</scp> surface using <scp>R</scp> aman piezospectroscopy. Journal of Raman Spectroscopy, 2018, 49, 1540-1551.	1.2	4
56	Microstructural Characterization of AA6061 Versus AA6061 HIP Bonded Cladding–Cladding Interface. Journal of Phase Equilibria and Diffusion, 2018, 39, 246-254.	0.5	17
5 <b>7</b>	Microstructure and mechanical behavior of the 3D printed Inconel 718: In-situ TEM study. Microscopy and Microanalysis, 2018, 24, 1942-1943.	0.2	2
58	A novel light diffuser based on the combined morphology of polymer networks and polymer balls in a polymer dispersed liquid crystals film. RSC Advances, 2018, 8, 21690-21698.	1.7	35
59	Nonelectric Sustaining Bistable Polymer Framework Liquid Crystal Films with a Novel Semirigid Polymer Matrix. ACS Applied Materials & Interfaces, 2018, 10, 22757-22766.	4.0	15
60	Unconventional High-Performance Laser Protection System Based on Dichroic Dye-Doped Cholesteric Liquid Crystals. Scientific Reports, 2017, 7, 42955.	1.6	12
61	Reprogrammable Assembly of Molecular Motor on Solid Surfaces via Dynamic Bonds. Small, 2017, 13, 1700480.	5.2	9
62	Strained W(Se <sub><i>x</i></sub> S <sub>1–<i>x</i></sub> ) <sub>2</sub> Nanoporous Films for Highly Efficient Hydrogen Evolution. ACS Energy Letters, 2017, 2, 1315-1320.	8.8	64
63	Periodically Patterned Au-TiO <sub>2</sub> Heterostructures for Photoelectrochemical Sensor. ACS Sensors, 2017, 2, 621-625.	4.0	86
64	Microstructural and crystallographic characteristics of modulated martensite, non-modulated martensite, and pre-martensitic tweed austenite in Ni-Mn-Ga alloys. Acta Materialia, 2017, 134, 93-103.	3.8	42
65	Overall Water Splitting with Room-Temperature Synthesized NiFe Oxyfluoride Nanoporous Films. ACS Catalysis, 2017, 7, 8406-8412.	5.5	91
66	NiS <sub>2</sub> /FeS Holey Film as Freestanding Electrode for Highâ€Performance Lithium Battery. Advanced Energy Materials, 2017, 7, 1701309.	10.2	99
67	Strengthening in hybrid alumina-titanium diboride aluminum matrix composites synthesized by ultrasonic assisted reactive mechanical mixing. Materials Science & Engineering A: Structural Materials: Properties, Microstructure and Processing, 2017, 702, 312-321.	2.6	21
68	Composition-dependent interdiffusion coefficient, reduced elastic modulus and hardness in γ-, γâ€2- and β-phases in the Ni-Al system. Journal of Alloys and Compounds, 2017, 727, 153-162.	2.8	25
69	Lithium Batteries: NiS <sub>2</sub> /FeS Holey Film as Freestanding Electrode for Highâ€Performance Lithium Battery (Adv. Energy Mater. 22/2017). Advanced Energy Materials, 2017, 7, .	10.2	0
70	Effect of a Polymercaptan Material on the Electro-Optical Properties of Polymer-Dispersed Liquid Crystal Films. Molecules, 2017, 22, 43.	1.7	16
71	A Study on the Electro-Optical Properties of Thiol-Ene Polymer Dispersed Cholesteric Liquid Crystal (PDChLC) Films. Molecules, 2017, 22, 317.	1.7	20
72	Enhanced Photoelectrocatalytic Reduction of Oxygen Using Au@TiO <sub>2</sub> Plasmonic Film. ACS Applied Materials & Interfaces, 2016, 8, 34970-34977.	4.0	52

Le Zhou

#	Article	IF	CITATIONS
73	Mechanical anomaly observed in Ni-Mn-Ga alloys by nanoindentation. Acta Materialia, 2016, 118, 54-63.	3.8	17
74	Thermally stable transparent sol–gel based active siloxane–oligomer materials with tunable high refractive index and dual reactive groups. RSC Advances, 2016, 6, 70825-70831.	1.7	17
75	Atomistic study on the interaction of nitrogen and Mg lattice and the nitride formation in nanocrystalline Mg alloys synthesized using cryomilling process. Acta Materialia, 2016, 115, 295-307.	3.8	7
76	Improvement of aging kinetics and precipitate size refinement in Mg–Sn alloys by hafnium additions. Materials Science & Engineering A: Structural Materials: Properties, Microstructure and Processing, 2016, 651, 854-858.	2.6	16
77	Multi-shape-memory effects in a wavelength-selective multicomposite. Journal of Materials Chemistry A, 2015, 3, 13953-13961.	5.2	57
78	Microstructural Development and Ternary Interdiffusion in Ni-Mn-Ga Alloys. Metallurgical and Materials Transactions A: Physical Metallurgy and Materials Science, 2015, 46, 5572-5587.	1.1	8
79	Nanostructured tungsten through cryogenic attrition. International Journal of Refractory Metals and Hard Materials, 2015, 52, 70-77.	1.7	2
80	Failure characteristics and mechanisms of EB-PVD TBCs with Pt-modified NiAl bond coats. Materials Science & Engineering A: Structural Materials: Properties, Microstructure and Processing, 2015, 637, 98-106.	2.6	15
81	Magnetocaloric response of non-stoichiometric Ni2MnGa alloys and the influence of crystallographic texture. Acta Materialia, 2015, 97, 245-256.	3.8	24
82	Martensitic transformation and mechanical properties of Ni49+xMn36–xIn15 (x=0, 0.5, 1.0, 1.5 and 2.0) alloys. Materials Science & Engineering A: Structural Materials: Properties, Microstructure and Processing, 2015, 646, 57-65.	2.6	14
83	Diffusion kinetics, mechanical properties, and crystallographic characterization of intermetallic compounds in the Mg–Zn binary system. Intermetallics, 2015, 67, 145-155.	1.8	47
84	Microstructural and Crystallographic Characterization of Ni2+x Mn1â^'x Ga Alloys (xÂ=Â0.14, 0.16, 0.19,) Tj ETQq 1, 239-246.	0 0 0 rgB 0.5	[  Overlock ] 4
85	Effects of Cr and Ni on interdiffusion and reaction between U and Fe–Cr–Ni alloys. Journal of Nuclear Materials, 2014, 451, 372-378.	1.3	12
86	Interdiffusion and reaction between Zr and Al alloys from 425° to 625°C. Intermetallics, 2014, 49, 154-162.	1.8	19
87	Sc-phthalocyanine sheet: Promising material for hydrogen storage. Applied Physics Letters, 2011, 99, .	1.5	32
88	Microstructure and Thermal Properties of Plasma Sprayed Thermal Barrier Coatings from Nanostructured YSZ. Journal of Thermal Spray Technology, 2010, 19, 1186-1194.	1.6	126
89	HOT-CORROSION BEHAVIOR OF THERMAL BARRIER COATED DZ125 SUPERALLOY EXPOSED TO ATOMIZED SEAWATER AND KEROSENE. International Journal of Modern Physics B, 2010, 24, 3155-3160.	1.0	0